

A Geometric Approach to Three-Dimensional Hipped Bipedal Robotic Walking

Aaron D. Ames, Robert D. Gregg and Mark W. Spong

Abstract—This paper presents a control law that results in stable walking for a three-dimensional bipedal robot with a hip. To obtain this control law, we utilize techniques from geometric reduction, and specifically a variant of Routhian reduction termed *functional Routhian reduction*, to effectively decouple the dynamics of the three-dimensional biped into its sagittal and lateral components. Motivated by the decoupling afforded by functional Routhian reduction, the control law we present is obtained by combining three separate control laws: the first shapes the potential energy of the sagittal dynamics of the biped to obtain stable walking gaits when it is constrained to the sagittal plane, the second shapes the total energy of the walker so that functional Routhian reduction can be applied to decoupling the dynamics of the walker for certain initial conditions, and the third utilizes an output zeroing controller to stabilize to the surface defining these initial conditions. We numerically verify that this method results in stable walking, and we discuss certain attributes of this walking gait.

I. INTRODUCTION

Bipedal robotic walking has been studied from a variety of perspectives (see [5], [6], [9] and [10] to name a few), but in most cases these studies have been limited to two-dimensional (2D) bipedal robots. There are some limited results related to three-dimensional (3D) bipeds, an interesting example of which is given in [4] and [7], but the general understanding of 3D bipedal walking is still extremely limited. Motivated by our previous results on *hipless* 3D bipeds, which allowed for the extension of 2D walking gaits to three dimensions through geometric reduction ([1] and [2]), we advocate a reduction-based approach to hipped bipedal walking.

The goal of this paper is to design a feedback control law for a 3D hipped bipedal robot that results in stable walking. In order to achieve this goal, we attempt to exploit the natural dynamics of the walker—this amounts to properly understanding the interplay between the sagittal and lateral components of bipedal walking. That is, in order to construct our control law, we must mathematically understand how to “decouple” the dynamics of a 3D biped into its sagittal and lateral components, which is done through the use of geometric reduction. Once it is understood how to appropriately separate the dynamics, we can design a control law for the 3D biped by combining controllers that (1) stabilize the

sagittal dynamics, (2) stabilize the lateral dynamics, and (3) combine these two controllers in the appropriate manner.

Fundamental to understanding the interplay between the lateral and sagittal dynamics of the considered 3D walker is a variant of Routhian reduction, termed *functional Routhian reduction*; this generalizes our previous functional Routhian reduction results in [2] to include off-diagonal elements in the inertia matrix which will occur in hipped bipeds and bipeds with non-zero link inertias. As with classical reduction, this form of reduction utilizes symmetries in a system, in the form of “cyclic” variables, to reduce the dimensionality of the system. Unlike classical reduction, this is done by setting the conserved quantities equal to an arbitrary function of the “cyclic” variables rather than a constant, i.e., there is a *functional conserved quantity*. This allows us to “control” the decoupling effect of geometric reduction through this function—a fact that will be fundamental in the construction of our control law.

The main control law presented in this paper is directed at applying functional Routhian reduction in a meaningful manner by combining three control laws:

First Control Law: Affects the sagittal dynamics of the biped by shaping the potential energy so that the 2D biped, obtained by constraining the 3D biped to the sagittal plane, has stable walking gaits.

Second Control Law: Shapes the total energy of the 3D biped so that functional Routhian reduction can be applied; moreover, the reduced system obtained by applying this form of reduction is exactly the 2D system after applying the first control law. Therefore, applying functional Routhian reduction to the 3D biped through the second control law decouples the sagittal and lateral dynamics, while allowing us to affect the lateral dynamics through our specific choice of the functional conserved quantity, for *certain initial conditions*.

Third Control Law: Stabilizes to the surface defining initial conditions for which the decoupling afforded by the second control law is valid. This is done by defining an output function that has the above initial conditions as its zero-level set, and stabilizing this output to zero through input-output linearization.

We are able to numerically verify that the control law presented in this paper results in stable walking, i.e., a locally exponentially stable periodic orbit. While this is certainly the most important aspect of this controller, other interesting

A. D. Ames is with the Control and Dynamical Systems Department, California Institute of Technology, Pasadena, CA 91125 ames@cds.caltech.edu

R. D. Gregg and M. W. Spong are with the Department of Electrical and Computer Engineering, University of Illinois at Urbana-Champaign, Urbana, IL 61801 rgregg@uiuc.edu, msspong@uiuc.edu

This work was partially supported by NSF Grant CMS-0510119.

behavior occurs as a byproduct of the techniques used to construct this control law. The most fascinating of these is that the periodic orbits we obtain are 1-periodic in the sagittal dynamics (as one would expect), but 2-periodic in the lateral dynamics (as one would hope); this is a result of the side-to-side swaying motion of the walker, which is a natural byproduct of the functional Routhian reduction. This seems to imply that the techniques we utilize capture a subtle, yet important, aspect of bipedal walking.

II. BIPEDAL MODEL

Hybrid systems are systems that display both continuous and discrete behavior and so bipedal walkers are naturally modeled by systems of this form; the continuous component consists of the dynamics dictated by the Lagrangian modeling this system, and the discrete component consists of the impact equations which instantaneously change the velocity of the system when the foot contacts the ground. This section, therefore, introduces the basic terminology of hybrid systems and introduces the hybrid model of the biped considered in this paper.

Definition 2.1: A simple hybrid control system is a tuple

$$\mathcal{H}\mathcal{C} = (D, U, G, R, f, g),$$

where

- $D \subseteq \mathbb{R}^n$ is a subset of \mathbb{R}^n called the *domain*,
- $U \subseteq \mathbb{R}^k$ is a set of *admissible controls*,
- $G \subset D$ is subset of D called the *guard*,
- $R : G \rightarrow D$ is a smooth map called the *reset map* (or *impact equations*),
- (f, g) is a *control system*, i.e., $\dot{x} = f(x) + g(x)u$.

A *simple hybrid system*¹ is a simple hybrid control system with $U = \{0\}$, i.e., a tuple: $\mathcal{H} = (D, G, R, f)$, where f is a vector field on D , i.e., $\dot{x} = f(x)$.

Hybrid flows. A *hybrid flow* of a hybrid system \mathcal{H} is a tuple $\chi^{\mathcal{H}} = (\Lambda, \mathcal{I}, \mathcal{C})$, where

- $\Lambda = \{0, 1, 2, \dots\} \subseteq \mathbb{N}$ is a finite or infinite indexing set.
- $\mathcal{I} = \{I_i\}_{i \in \Lambda}$ is a *hybrid interval* where $I_i = [\tau_i, \tau_{i+1}]$ if $i, i+1 \in \Lambda$ and $I_{N-1} = [\tau_{N-1}, \tau_N]$ or $[\tau_{N-1}, \tau_N]$ or $[\tau_{N-1}, \infty)$ if $|\Lambda| = N$, N finite. Here, $\tau_i, \tau_{i+1}, \tau_N \in \mathbb{R}$ and $\tau_i \leq \tau_{i+1}$.
- $\mathcal{C} = \{c_i\}_{i \in \Lambda}$ is a collection of integral curves of f , i.e., $\dot{c}_i(t) = f(c_i(t))$ for all $i \in \Lambda$.

We require that for every $i, i+1 \in \Lambda$,

- (i) $c_i(\tau_{i+1}) \in G$,
- (ii) $R(c_i(\tau_{i+1})) = c_{i+1}(\tau_{i+1})$.

The *initial condition* for the hybrid flow is $c_0(\tau_0)$.

¹It is important to note that simple hybrid systems correspond to systems with impulsive effects (see [6] and [10]) and vice versa. Specifically to a simple hybrid system, there is the associated system with impulsive effects of the form:

$$\Sigma : \begin{cases} \dot{x} = f(x) & x \in D \setminus G \\ x^+ = R(x^-) & x^- \in G \end{cases}$$

Hybrid periodic orbits. In the context of bipedal robots, we are interested in discussing walking gaits and stable walking gaits—these correspond to periodic orbits and stable periodic orbits, respectively, of different periods. For example, in the context of hipped bipedal walking, we will be interested in 2-periodic orbits due to the natural side-to-side swaying motion of a 3D bipedal walker.

A hybrid flow $\chi^{\mathcal{H}} = (\Lambda, \mathcal{I}, \mathcal{C})$ of \mathcal{H} is *k-periodic* if

- $\Lambda = \mathbb{N}$,
- $\lim_{i \rightarrow \infty} \tau_i = \infty$,
- $c_i(\tau_i) = c_{i+k}(\tau_{i+k})$ for all $i \in \Lambda$.

A *hybrid k-periodic orbit* $\mathcal{O} \subset D$ is a subset of D such that

$$\mathcal{O} = \bigcup_{i \in \mathbb{N}} \{c_i(t) : t \in I_i\}$$

for some *k*-periodic hybrid flow $\chi^{\mathcal{H}}$.

As is standard, denote the distance between a point x and a set Y by $d(x, Y) = \inf_{y \in Y} \|x - y\|$. A hybrid *k*-periodic orbit \mathcal{O} is (*locally*) *exponentially stable* if there exists constants $M > 0$, $\alpha > 0$ and $\delta > 0$ such that for all hybrid flows $\chi^{\mathcal{H}}$ with $d(c_0(\tau_0), \mathcal{O}) < \delta$,

$$d(c_i(t), \mathcal{O}) \leq M e^{-\alpha(t-\tau_0)} d(c_0(\tau_0), \mathcal{O})$$

for all $t \in I_i$ and $i \in \Lambda$.

Poincaré map. In order to establish the stability of *k*-periodic orbits, we will use the standard technique of studying the corresponding Poincaré map (cf. [10]). In particular, taking G to be the Poincaré section, one obtains the Poincaré map, $P : G \rightarrow G$, which is a partial map defined by:

$$P(z) = c(\tau(z)),$$

where $c(t)$ is the solution to $\dot{x} = f(x)$ with $c(0) = R(z)$ and $\tau(z)$ is the *time-to-impact* function (again, see [10]). In particular, if z^* is a *k*-fixed point of P (under suitable assumptions on z^* , G , and the transversality of \mathcal{O} and G) a *k*-periodic orbit \mathcal{O} with $z^* \in \mathcal{O}$ is locally exponentially stable iff P^k is locally exponentially stable (as a discrete-time dynamical system, $z_{i+1} = P(z_i)$).

Although it is not possible to explicitly compute the Poincaré map, one can compute a numerical approximation of this map through simulation and thereby test its stability numerically. This gives a concrete method for practically testing the stability of periodic orbits (see [5] for a nice tutorial on numerically computing the eigenvalues of the Poincaré map).

3D biped model. The model of interest is a controlled bipedal robot with a hip and splayed legs that walks on flat ground in three dimensions (see Figure 1), from which we will explicitly construct the hybrid control system:

$$\mathcal{H}\mathcal{C}_{3D} = (D_{3D}, U_{3D}, G_{3D}, R_{3D}, f_{3D}, g_{3D}).$$

The techniques utilized in the construction of this hybrid system are explained in further detail in [2].

The configuration space for the 3D biped is taken to be $Q_{3D} = \mathbb{T}^2 \times \mathbb{S}^1$, with coordinates $q = (\theta^T, \varphi)^T$, where $\theta = (\theta_{ns}, \theta_s)^T$ is the vector of sagittal-plane variables as in

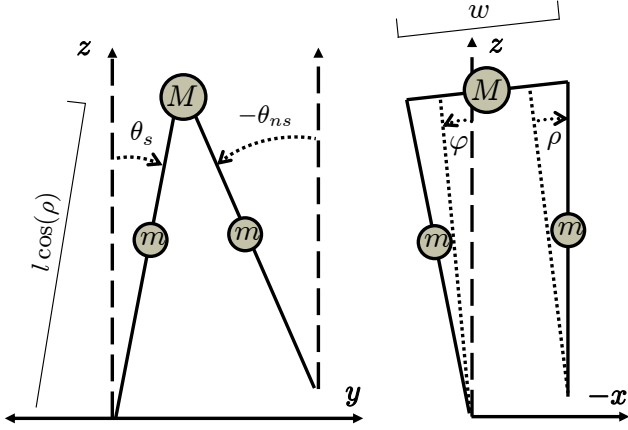


Fig. 1. The sagittal and lateral planes of a three-dimensional bipedal robot.

the 2D compass-gait model and φ is the lean (or roll) from vertical; we will work in these coordinates throughout the course of the paper. Note that the hip width w , leg length l , and leg splay angle ρ are held constant.

The domain and guard are constructed from the constraint that the non-stance (swing) foot is not allowed to pass through the ground, i.e., by utilizing the unilateral constraint function:

$$H_{3D}(q) = l(\cos(\theta_s) - \cos(\theta_{ns}))\cos(\varphi) - (w + 2l\sin(\rho))\sin(\varphi)$$

which gives the height of the non-stance foot above the ground. In particular, the domain D_{3D} is given by requiring that the height of the swing foot always be positive:

$$D_{3D} = \left\{ \begin{pmatrix} q \\ \dot{q} \end{pmatrix} \in TQ_{3D} : H_{3D}(q) \geq 0 \right\}$$

We put no restrictions on the set of admissible controls except that they can only directly affect the angular accelerations. Therefore, $U_{3D} = \mathbb{R}^3$.

The guard G_{3D} is the subset of the domain corresponding to the set of configurations in which the height of the swing foot is zero and infinitesimally decreasing. That is,

$$G_{3D} = \left\{ \begin{pmatrix} q \\ \dot{q} \end{pmatrix} \in TQ_{3D} : H_{3D}(q) = 0, \left(\frac{\partial H_{3D}(q)}{\partial q} \right)^T \dot{q} < 0 \right\}.$$

The reset map R_{3D} is given by:

$$R_{3D}(q, \dot{q}) = \begin{pmatrix} S_\theta & 0 & 0 & 0 \\ 0 & 1 & 0 & 0 \\ 0 & 0 & P_\theta(\theta) & p_{\theta, \varphi}(\theta) \\ 0 & 0 & P_{\varphi, \theta}(\theta) & p_\varphi(\theta) \end{pmatrix} \begin{pmatrix} \theta \\ \varphi \\ \dot{\theta} \\ \dot{\varphi} \end{pmatrix}$$

where $p_\varphi(\theta)$, $P_{\varphi, \theta}(\theta)$, $p_{\theta, \varphi}(\theta)$ and $P_\theta(\theta)$ are computed symbolically using Mathematica and the procedures outlined in [2] and [6]; the length of these equations prevent them from being included in this paper. Also, note that the signs

of w and ρ are flipped during impact to model the change in stance leg.

Finally, the dynamics for $\mathcal{H}\mathcal{C}_{3D}$ are obtained from the Euler-Lagrange equations in the standard way. Specifically, the Lagrangian describing this system is:

$$L_{3D}(q, \dot{q}) = \frac{1}{2} \dot{q}^T M_{3D}(q) \dot{q} - V_{3D}(q),$$

with

$$M_{3D}(q) = \begin{pmatrix} M_\theta(\theta) & M_{\varphi, \theta}(\theta)^T \\ M_{\varphi, \theta}(\theta) & m_\varphi(\theta) \end{pmatrix}, \quad (1)$$

where $M_{3D}(q)$ is the inertial matrix and $V_{3D}(q)$ is the potential energy (these can be found in Table I). Using the controlled Euler-Lagrange equations, the dynamics for the walker are given by:

$$M_{3D}(q)\ddot{q} + C_{3D}(q, \dot{q})\dot{q} + N_{3D}(q) = B_{3D}u,$$

where $C_{3D}(q, \dot{q})$ is the Coriolis matrix, $N_{3D} = \frac{\partial V_{3D}(q)}{\partial q}$, and

$$B_{3D} = \begin{pmatrix} B_\theta & 0 \\ 0 & 1 \end{pmatrix}.$$

In addition, we assume that B_{3D} is invertible. These equations yield the control system:

$$\begin{aligned} f_{3D}(q, \dot{q}) &= \begin{pmatrix} \dot{q} \\ M_{3D}(q)^{-1} (-C_{3D}(q, \dot{q})\dot{q} - N_{3D}(q)) \end{pmatrix} \\ g_{3D}(q, \dot{q}) &= \begin{pmatrix} 0_{3 \times 3} \\ M_{3D}(q)^{-1} B_{3D} \end{pmatrix}, \end{aligned}$$

where $0_{3 \times 3}$ is a 3×3 matrix of zeros.

III. FUNCTIONAL ROUTHIAN REDUCTION

In this section, we introduce a variant of standard Routhian reduction (see [8] for a detailed introduction, and [3] for a brief introduction), termed *functional Routhian reduction*. This type of geometric reduction allows for one to reduce the dimensionality of dynamical systems obtained from ‘‘almost-cyclic’’ Lagrangians. Moreover, considering such Lagrangians allows one to affect the behavior of the reduced (‘‘cyclic’’) variables. This type of reduction, therefore, will be fundamental in the construction of our control law.

Almost-Cyclic Lagrangians. Consider the case when the configuration space $Q = S \times \mathbb{S}^1$, where S is called the *shape space*. We denote an element $q \in Q$ by $q = (\theta^T, \varphi)^T$, where $\theta \in S$ and $\varphi \in \mathbb{S}^1$.

In the context of bipedal walking, we are interested in Lagrangians of a very special form. We say that a Lagrangian $L_\lambda : TS \times T\mathbb{S}^1 \rightarrow \mathbb{R}$ is *almost-cyclic* if, in coordinates, it has the form:

$$L_\lambda(\theta, \varphi, \dot{\theta}, \dot{\varphi}) = \frac{1}{2} \begin{pmatrix} \dot{\theta}^T & \dot{\varphi} \end{pmatrix} M_\lambda(\theta) \begin{pmatrix} \dot{\theta} \\ \dot{\varphi} \end{pmatrix} - W_\lambda(\theta, \varphi, \dot{\theta}) - V_\lambda(\theta, \varphi), \quad (2)$$

where

$$M_\lambda(\theta) = \begin{pmatrix} M_\theta(\theta) + \frac{M_{\varphi, \theta}(\theta)^T M_{\varphi, \theta}(\theta)}{m_\varphi(\theta)} & M_{\varphi, \theta}(\theta)^T \\ M_{\varphi, \theta}(\theta) & m_\varphi(\theta) \end{pmatrix},$$

$$\begin{aligned}
M_\theta(\theta) &= \begin{pmatrix} \frac{l^2 m}{4} (\cos(\rho) - 2)^2 & \frac{l^2 m}{2} (\cos(\rho) - 2) \cos(\theta_s - \theta_{ns}) \\ \frac{l^2 m}{2} (\cos(\rho) - 2) \cos(\theta_s - \theta_{ns}) & \frac{l^2}{8} (9m + 4M + (m + 4M) \cos(2\rho)) \end{pmatrix} & S_\theta &= \begin{pmatrix} 0 & 1 \\ 1 & 0 \end{pmatrix} \\
V_\theta(\theta) &= \frac{gl}{2} (m(\cos(\rho) - 2) \cos(\theta_{ns}) + (2m + (m + 2M) \cos(\rho)) \cos(\theta_s)) & B_\theta &= \begin{pmatrix} -1 & 0 \\ 1 & 1 \end{pmatrix} \\
m_\varphi(\theta) &= \frac{1}{16} (2l^2(19m + 6M) + 4(4m + M)w^2 + l(lm(9 \cos(2\theta_{ns}) + 16 \cos(\theta_{ns})(\cos(\theta_s)(\cos(\rho) - 2) - \cos(\rho) \cos(\theta_{ns}))) \\
&\quad + l(9m + 4M) \cos(2\theta_s) + l \cos(2\rho)(m \cos(2\theta_{ns}) - 18m - 4M + (m + 4M) \cos(2\theta_s)) + 16(3m + M)w \sin(\rho)) \\
M_{\varphi,\theta}(\theta) &= \left(\frac{1}{4} lm(\cos(\rho) - 2)(2w + 3l \sin(\rho)) \sin(\theta_{ns}) \quad \frac{1}{4} l(4mw + 6lm \sin(\rho) + \cos(\rho)(2Mw + l(m + 4M) \sin(\rho))) \sin(\theta_s) \right) \\
V_{3D}(\theta, \varphi) &= V_\theta(\theta) \cos(\varphi) - \frac{g}{2} (2m + M)(w + 2l \sin(\rho)) \sin(\varphi)
\end{aligned}$$

TABLE I
ADDITIONAL EQUATIONS FOR $\mathcal{H}\mathcal{C}_{3D}$ AND $\mathcal{H}\mathcal{C}_{2D}$

$$\begin{aligned}
W_\lambda(\theta, \varphi, \dot{\theta}) &= \frac{\lambda(\varphi)}{m_\varphi(\theta)} M_{\varphi,\theta}(\theta) \dot{\theta}, \\
V_\lambda(\theta, \varphi) &= V_{\text{fct}}(\theta) - \frac{1}{2} \frac{\lambda(\varphi)^2}{m_\varphi(\theta)},
\end{aligned}$$

for some function $\lambda : \mathbb{S}^1 \rightarrow \mathbb{R}$. Here, for all θ , $M_\theta(\theta) \in \mathbb{R}^{n \times n}$ (with $n = \dim(S)$) and $m_\varphi(\theta) \in \mathbb{R}$ are symmetric and positive definite.

Momentum maps. Fundamental to reduction is the notion of a momentum map $J : TQ \rightarrow \mathbb{R}$, which makes explicit the conserved quantities in the system. In the framework we are considering here,

$$J(\theta, \varphi, \dot{\theta}, \dot{\varphi}) = \frac{\partial L_\lambda}{\partial \dot{\varphi}}(\theta, \varphi, \dot{\theta}, \dot{\varphi}) = M_{\varphi,\theta}(\theta) \dot{\theta} + m_\varphi(\theta) \dot{\varphi}.$$

In the case of standard Routhian reduction, one sets the momentum map equal to a constant $\mu \in \mathbb{R}$; this defines the conserved quantities of the system. In our framework, we will breach this convention and set J equal to a function $\lambda(\varphi)$: this motivates the name *functional Routhian reduction*.

Functional Routhians. For an almost-cyclic Lagrangian L_λ as given in (2), define the corresponding *functional Routhian* $L_{\text{fct}} : TS \rightarrow \mathbb{R}$ by:

$$L_{\text{fct}}(\theta, \dot{\theta}) = \left[L_\lambda(\theta, \varphi, \dot{\theta}, \dot{\varphi}) - \lambda(\varphi) \dot{\varphi} \right] \Big|_{J(\theta, \varphi, \dot{\theta}, \dot{\varphi}) = \lambda(\varphi)}$$

Because $J(\theta, \varphi, \dot{\theta}, \dot{\varphi}) = \lambda(\varphi)$ implies that

$$\dot{\varphi} = \frac{1}{m_\varphi(\theta)} (\lambda(\varphi) - M_{\varphi,\theta}(\theta) \dot{\theta}), \quad (3)$$

by direct calculation the functional Routhian is given by:

$$L_{\text{fct}}(\theta, \dot{\theta}) = \frac{1}{2} \dot{\theta}^T M_\theta(\theta) \dot{\theta} - V_{\text{fct}}(\theta).$$

We can relate solutions of the Lagrangian vector field $f_{L_{\text{fct}}}$ to solutions of the Lagrangian vector field f_{L_λ} and vice versa (in a way analogous to the classical Routhian reduction result, see [8]). This observation is the main theoretical result of this paper.

Theorem 1: *Let L_λ be an almost-cyclic Lagrangian, and L_{fct} the corresponding functional Routhian. Then*

$(\theta(t), \varphi(t), \dot{\theta}(t), \dot{\varphi}(t))$ is a solution to the vector field f_{L_λ} on $[t_0, t_F]$ with

$$\dot{\varphi}(t_0) = \frac{1}{m_\varphi(\theta(t_0))} (\lambda(\varphi(t_0)) - M_{\varphi,\theta}(\theta(t_0)) \dot{\theta}(t_0)), \quad (4)$$

if and only if $(\theta(t), \dot{\theta}(t))$ is a solution to the vector field $f_{L_{\text{fct}}}$ and $(\varphi(t), \dot{\varphi}(t))$ satisfies:

$$\dot{\varphi}(t) = \frac{1}{m_\varphi(\theta(t))} (\lambda(\varphi(t)) - M_{\varphi,\theta}(\theta(t)) \dot{\theta}(t)). \quad (5)$$

The proof of this theorem is rather long and involved, so we include it in the Appendix. Note that Theorem 1 is a generalization of the functional reduction theorem first introduced and utilized in [2].

IV. CONTROL LAW CONSTRUCTION

In this section, we introduce our control law for the 3D biped introduced in Section II. This control law is obtained by combining three separate control laws: the first control law acts on the sagittal dynamics of the walker in a way analogous to the controlled symmetries control law used for 2D walkers, the second control law transforms the Lagrangian of the 3D walker into an almost-cyclic Lagrangian, and the third control law utilizes zero dynamics techniques to stabilize to the set of initial conditions specified in Theorem 1. The end result of combining these control laws is a controller that results in stable 3D bipedal walking—the specific behavior obtained through this control law will be discussed in the next section.

Reduced dynamics controller. The first controller affects the dynamics of the 3D biped's sagittal plane by shaping the potential energy of the Lagrangian describing these dynamics. The motivation for this control law is the standard controlled symmetries method of [12] to achieve walking on flat ground.

We begin by considering the sagittal dynamics of the 3D biped. These dynamics consist of a configuration space $Q_{2D} = \mathbb{T}^2$ with coordinates $\theta = (\theta_{ns}, \theta_s)^T$, where θ_{ns} is the angle of the non-stance leg from vertical and θ_s is the angle of the stance leg from vertical (see Figure 1), together with a Lagrangian given by:

$$L_{2D}(\theta, \dot{\theta}) = \frac{1}{2} \dot{\theta}^T M_\theta(\theta) \dot{\theta} - V_\theta(\theta),$$

where $M_\theta(\theta)$ and $V_\theta(\theta)$ are given in Table I.

The dynamics for the planar system are again obtained from the Euler-Lagrange equations. Specifically, the equations of motion are given by:

$$M_\theta(\theta)\ddot{\theta} + C_\theta(\theta, \dot{\theta})\dot{\theta} + N_\theta(\theta) = B_\theta u.$$

These equations yield the control system (f_{2D}, g_{2D}) as in the case of the full-order bipedal walker.

We can view the dynamics of the 2D subsystem as the continuous portion of a hybrid system modeling a 2D walker, i.e., a hybrid control system

$$\mathcal{H}\mathcal{C}_{2D} = (D_{2D}, U_{2D}, G_{2D}, R_{2D}, f_{2D}, g_{2D})$$

where

$$\begin{aligned} D_{2D} &= \left\{ \begin{pmatrix} \theta \\ \dot{\theta} \end{pmatrix} \in TQ_{2D} : H_{2D}(\theta) \geq 0 \right\}, \\ G_{2D} &= \left\{ \begin{pmatrix} \theta \\ \dot{\theta} \end{pmatrix} \in TQ_{2D} : H_{2D}(\theta) = 0, \right. \\ &\quad \left. \left(\frac{\partial H_{2D}(\theta)}{\partial \theta} \right)^T \dot{\theta} < 0 \right\}, \end{aligned}$$

with $H_{2D}(\theta) = \cos(\theta_s) - \cos(\theta_{ns})$, $U_{2D} = \mathbb{R}^2$, and

$$R_{2D}(\theta, \dot{\theta}) = \begin{pmatrix} S_\theta \theta \\ P_\theta(\theta) \dot{\theta} \end{pmatrix},$$

where S_θ and $P_\theta(\theta)$ are the same as in the 3D bipedal model.

The hybrid control system $\mathcal{H}\mathcal{C}_{2D}$ is similar, but not equivalent, to the typical 2D compass-gait walker (cf. [1], [2] and [5]), since the splayed legs affect the height of the planar robot—this observation motivates the control law to be introduced. That is, we utilize controlled symmetries of [12] by “rotating the world” via a group action in order to shape the potential energy of L_{2D} to obtain stable walking gaits on flat ground for $\mathcal{H}\mathcal{C}_{2D}$.

Consider the group action $\Psi : \mathbb{S}^1 \times Q_{2D} \rightarrow Q_{2D}$ denoted by:

$$\Psi_\gamma(\theta) := \begin{pmatrix} \theta_{ns} - \gamma \\ \theta_s - \gamma \end{pmatrix},$$

for slope angle $\gamma \in \mathbb{S}^1$. Using this, define the following feedback control law:

$$u = K_R^\gamma(\theta) = B_\theta^{-1} (N_\theta(\theta) - N_\theta(\Psi_\gamma(\theta))). \quad (6)$$

Applying this control law to the control system (f_{2D}, g_{2D}) yields the dynamical system:

$$f_{2D}^\gamma(\theta, \dot{\theta}) := f_{2D}(\theta, \dot{\theta}) + g_{2D}(\theta, \dot{\theta})K_R^\gamma(\theta).$$

which is just the vector field associated to the Lagrangian:

$$L_{2D}^\gamma(\theta, \dot{\theta}) = \frac{1}{2} \dot{\theta}^T M_\theta(\theta) \dot{\theta} - V_\theta(\Psi_\gamma(\theta)). \quad (7)$$

As with the standard compass-gait biped, it is easy to verify that there exists a γ (in fact, a range of γ) such that the hybrid system

$$\mathcal{H}\mathcal{C}_{2D}^\gamma := (D_{2D}, G_{2D}, R_{2D}, f_{2D}^\gamma)$$

has a stable walking gait, i.e., a stable hybrid periodic orbit.

Lagrangian shaping controller. The goal of this controller is to shape both the kinetic and potential energy of L_{3D} so as to render it “almost-cyclic.”

Consider the following almost-cyclic Lagrangian:

$$\begin{aligned} L_\alpha^\gamma(\theta, \varphi, \dot{\theta}, \dot{\varphi}) &= \\ &= \frac{1}{2} \begin{pmatrix} \dot{\theta}^T & \dot{\varphi} \end{pmatrix} M_\alpha(\theta) \begin{pmatrix} \dot{\theta} \\ \dot{\varphi} \end{pmatrix} - W_\alpha(\theta, \varphi, \dot{\theta}) - V_\alpha^\gamma(\theta, \varphi), \end{aligned} \quad (8)$$

where

$$M_\alpha(\theta) = \begin{pmatrix} M_\theta(\theta) + \frac{M_{\varphi, \theta}(\theta)^T M_{\varphi, \theta}(\theta)}{m_\varphi(\theta)} & M_{\varphi, \theta}(\theta)^T \\ M_{\varphi, \theta}(\theta) & m_\varphi(\theta) \end{pmatrix}$$

$$W_\alpha(\theta, \varphi, \dot{\theta}) = -\frac{\alpha\varphi}{m_\varphi(\theta)} M_{\varphi, \theta}(\theta) \dot{\theta}$$

$$V_\alpha^\gamma(\theta, \varphi) = V_\theta(\Psi_\gamma(\theta)) - \frac{1}{2} \frac{\alpha^2 \varphi^2}{m_\varphi(\theta)}$$

with $M_{\varphi, \theta}(\theta)$, $M_\theta(\theta)$, and $m_\varphi(\theta)$ as defined in (1) – the last two are positive definite since $M_{3D}(q) > 0$. Note that for this almost-cyclic Lagrangian, we have taken $\lambda(\varphi) = -\alpha\varphi$ and $V_{\text{fct}}(\theta) = V_\theta(\Psi_\gamma(\theta))$. It follows that the functional Routhian associated with this cyclic Lagrangian is L_{2D}^γ as given in (7).

Now we can define a feedback control law that transforms L_{3D} to L_α^γ . In particular, let

$$\begin{aligned} u &= K_S^{\alpha, \gamma}(q, \dot{q}) := B_{3D}^{-1} (C_{3D}(q, \dot{q})\dot{q} + N_{3D}(q) \\ &\quad + M_{3D}(q)M_\alpha(q)^{-1}(-C_\alpha(q, \dot{q})\dot{q} - N_\alpha^\gamma(q))), \end{aligned} \quad (9)$$

where $C_\alpha(q, \dot{q})$ is the shaped Coriolis matrix and $N_\alpha^\gamma = \frac{\partial V_\alpha^\gamma(q)}{\partial q}$. Note that this control law implicitly uses the first control law. Applying this to the control system (f_{3D}, g_{3D}) yields the dynamic system:

$$f_{3D}^{\alpha, \gamma}(q, \dot{q}) := f_{3D}(q, \dot{q}) + g_{3D}(q, \dot{q})K_S^{\alpha, \gamma}(q, \dot{q}), \quad (10)$$

which is just the vector field associated to the Lagrangian L_α^γ . Moreover, as a result of Theorem 1, we have the following relationship between the behavior of $f_{3D}^{\alpha, \gamma}$ and f_{2D}^γ :

Proposition 4.1: $(\theta(t), \varphi(t), \dot{\theta}(t), \dot{\varphi}(t))$ is a solution to the vector field $f_{3D}^{\alpha, \gamma}$ on $[t_0, t_F]$ with

$$\dot{\varphi}(t_0) = \frac{-1}{m_\varphi(\theta(t_0))} (\alpha\varphi(t_0) + M_{\varphi, \theta}(\theta(t_0))\dot{\theta}(t_0)), \quad (11)$$

if and only if $(\theta(t), \dot{\theta}(t))$ is a solution to the vector field f_{2D}^γ and $(\varphi(t), \dot{\varphi}(t))$ satisfies:

$$\dot{\varphi}(t) = \frac{-1}{m_\varphi(\theta(t))} (\alpha\varphi(t) + M_{\varphi, \theta}(\theta(t))\dot{\theta}(t)). \quad (12)$$

This result implies that for certain initial conditions, i.e., those satisfying (11), the dynamics of $\mathcal{H}\mathcal{C}_{3D}$ can be effectively decoupled into the sagittal and lateral dynamics by utilizing the control law $K_S^{\alpha, \gamma}$. Moreover, the lateral dynamics must satisfy the constraint (12), i.e., they evolve in a very specific fashion. It will be shown in the simulation section that this behavior is beneficial, but first we must discuss how to handle conditions that do not satisfy (11).

Zero dynamics controller. The decoupling effect of Proposition 4.1 can only be enjoyed when (11) is satisfied. Since most initial conditions will not satisfy this constraint, we will use the classical method of output linearization in non-linear systems to stabilize to the surface defined by this constraint (see [11] for the continuous case and [6], [10] for the hybrid analogue).

Before introducing the third control law, we define a new hybrid control system that implicitly utilizes the first two control laws. Specifically, let

$$\mathcal{H}\mathcal{C}_{3D}^{\alpha,\gamma} = (D_{3D}, \mathbb{R}, G_{3D}, R_{3D}, f_{3D}^{\alpha,\gamma}, g_{3D}^{\alpha,\gamma})$$

where D_{3D} , G_{3D} and R_{3D} are defined as for $\mathcal{H}\mathcal{C}_{3D}$. The control system $(f_{3D}^{\alpha,\gamma}, g_{3D}^{\alpha,\gamma})$ is given by applying the control law

$$u = K_S^{\alpha,\gamma}(q, \dot{q}) + \begin{pmatrix} 0 & 0 & 1 \end{pmatrix}^T v$$

to the control system (f_{3D}, g_{3D}) , where $v \in \mathbb{R}$. In particular, $f_{3D}^{\alpha,\gamma}$ is given as in (10) and

$$g_{3D}^{\alpha,\gamma}(q, \dot{q}) = \begin{pmatrix} 0 & 0 & 1 \end{pmatrix}^T g_{3D}(q, \dot{q}).$$

Motivated by our desire to satisfy (11), let

$$h(q, \dot{q}) := \dot{\varphi} + \frac{1}{m_\varphi(\theta)}(\alpha\varphi + M_{\varphi,\theta}(\theta)\dot{\theta}).$$

The main idea in the construction of the third control law is that we would like to drive $h(q, \dot{q})$ to zero, i.e., we would like to drive the system to the surface

$$\mathcal{Z} = \left\{ \begin{pmatrix} q \\ \dot{q} \end{pmatrix} \in TQ_{3D} : h(q, \dot{q}) = 0 \right\}.$$

With this in mind, and motivated by the standard method for driving an output function to zero in a nonlinear control system, we define the following feedback control law:

$$\begin{aligned} v &= K_Z^{\epsilon,\alpha,\gamma}(q, \dot{q}) \\ &:= \frac{-1}{L_{g_{3D}^{\alpha,\gamma}} h(q, \dot{q})} \left(L_{f_{3D}^{\alpha,\gamma}} h(q, \dot{q}) + \frac{1}{\epsilon} h(q, \dot{q}) \right), \end{aligned}$$

where $L_{g_{3D}^{\alpha,\gamma}} h(q, \dot{q})$ is the Lie derivative of h with respect to $g_{3D}^{\alpha,\gamma}$ and $L_{f_{3D}^{\alpha,\gamma}} h(q, \dot{q})$ is the Lie derivative of h with respect to $f_{3D}^{\alpha,\gamma}$. Note that we know $K_Z^{\epsilon,\alpha,\gamma}$ is well-defined since

$$L_{g_{3D}^{\alpha,\gamma}} h(q, \dot{q}) = \frac{1}{m_\varphi(\theta)},$$

and $m_\varphi(\theta) > 0$ by the positive definiteness of $M_{3D}(\theta)$.

Utilizing the feedback control law $K_Z^{\epsilon,\alpha,\gamma}$, we obtain a new hybrid system:

$$\mathcal{H}_{3D}^{\epsilon,\alpha,\gamma} := (D_{3D}, G_{3D}, R_{3D}, f_{3D}^{\epsilon,\alpha,\gamma}),$$

where

$$f_{3D}^{\epsilon,\alpha,\gamma}(q, \dot{q}) := f_{3D}^{\alpha,\gamma}(q, \dot{q}) + g_{3D}^{\alpha,\gamma}(q, \dot{q})K_S^{\epsilon,\alpha,\gamma}(q, \dot{q}).$$

Note that ϵ , α and γ can be thought of as control gains, as long as they are chosen so that $\epsilon > 0$, $\alpha > 0$, and γ such that \mathcal{H}_{2D}^γ has a stable periodic orbit. We now proceed to examine the behavior of $\mathcal{H}_{3D}^{\epsilon,\alpha,\gamma}$.

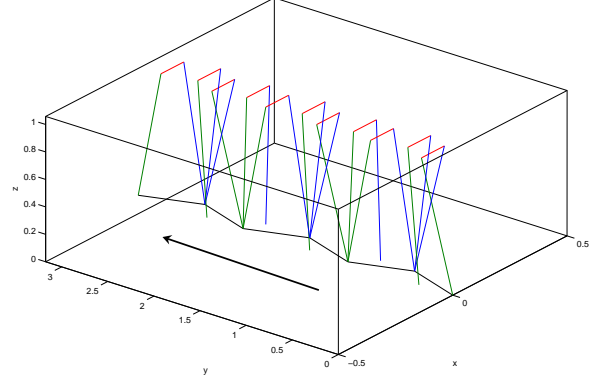


Fig. 2. A walking gait for the 3D biped.

V. SIMULATION RESULTS & CONCLUDING REMARKS

The main result of this paper is that the control law presented in the previous section results in stable hipped 3D bipedal walking—this will be demonstrated numerically.

The bipedal model of interest has hip width $w = 0.1$, leg length $l = 1$, and leg splay angle $\rho = 0.0188$. The control gains for $K_Z^{\epsilon,\alpha,\gamma}$ are chosen to be $\epsilon = \frac{1}{5}$ (to provide for sufficiently-fast convergence to \mathcal{Z}), $\alpha = 10$ (to maintain a dynamic upright posture) and $\gamma = \pi/50$ (so that the 2D system has a stable walking gait). It will be seen that the biped will naturally sway from side-to-side, so we first search for a 2-periodic orbit \mathcal{O}_{3D} , or a 2-periodic fixed point of the Poincaré map, which one can verify is given by:

$$\begin{pmatrix} \theta^* \\ \varphi^* \\ \dot{\theta}^* \\ \dot{\varphi}^* \end{pmatrix} \approx \begin{pmatrix} 0.2885 \\ -0.2877 \\ -0.0034 \\ -1.9708 \\ -1.5986 \\ 0.0360 \end{pmatrix}.$$

Therefore, it only remains to check that this two-periodic orbit is stable. This is done by numerically computing the eigenvalues of the Poincaré map. The magnitudes of these eigenvalues are given by: 0.2918, 0.2918, 0.2961, 0.0082, 0.0001, 0.0217. Therefore, we have numerically verified that \mathcal{O}_{3D} is a locally exponentially stable 2-periodic orbit; the 2-periodic orbit can be seen in Figure 3 and the walking gait corresponding to the orbit can be seen in Figure 2. We will briefly discuss the attributes of this gait.

We begin by noting that analytically proving the stability of this walking gait does not currently seem possible, or is extremely difficult. This is a common occurrence when studying bipedal walkers, although there has been some success in the case of hipless 3D bipedal robots—given 2D walking gaits, the stability of 3D walking gaits can be proven analytically using hybrid block-diagonal functional Routhian reduction and hybrid zero dynamics (cf. [1]). While the aforementioned method is very similar to the one proposed in this paper, adding a hip to the biped prevents the straightforward extension of these ideas—the necessary condition

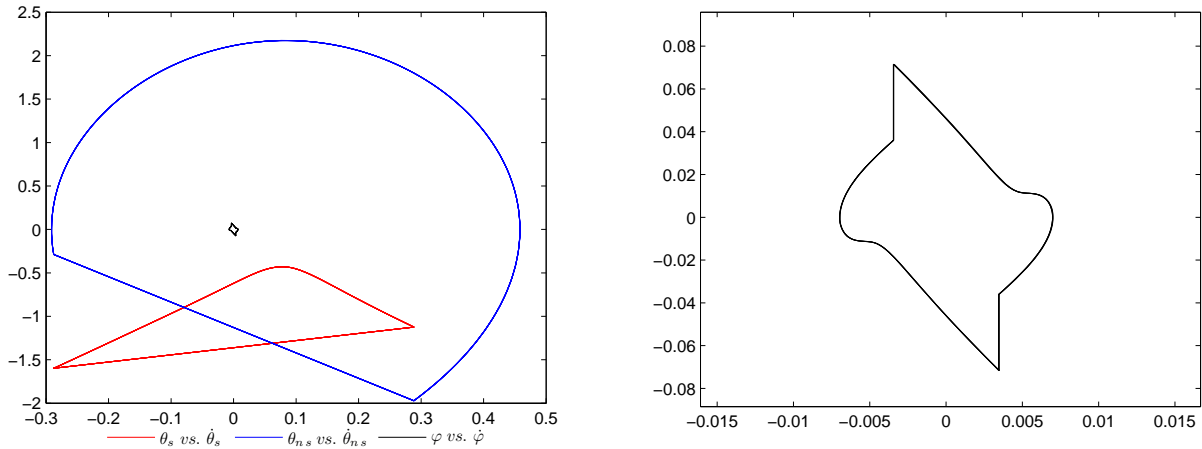


Fig. 3. A stable 3D limit cycle of the biped (left), and a zoomed view of the lateral-plane $(\varphi, \dot{\varphi})$ limit cycle (right).

that the conserved momentum quantity holds through the impact equations, i.e. $h(q, \dot{q}) = h(R_{3D}(q, \dot{q}))$, is violated. Consequently, there is not a hybrid-invariant surface \mathcal{Z} by which the hybrid zero dynamics theorem of [10] can be applied.

The control law presented in this paper was designed to be robust to the perturbations of h that occur through the impacts. In particular, at every impact the zero dynamics controller will correct the introduced error $e(q, \dot{q}) = h(q, \dot{q}) - h(R_{3D}(q, \dot{q}))$, driving $h(q, \dot{q})$ to zero so that the conditions of Proposition 4.1 are satisfied. When this error is introduced, the decoupling of the 2D limit cycle is violated until the zero dynamics correct to the conserved quantity. This decoupling perturbs the 2D limit cycle, but we argue that for sufficiently small ϵ (and thus sufficiently fast convergence to the conserved quantity surface), the perturbation will be within the 2D cycle's basin of attraction after every step. This argument is supported by the numerical analysis of the periodic orbit.

Aside from the robustness introduced through the zero dynamics controller, the Lagrangian shaping controller and the corresponding reduced dynamics controller also have an interesting effect on the behavior of the biped. The first is that the sagittal component of the 2-periodic orbit (see Figure 3) looks very similar to the standard compass-gait biped's periodic orbit. This indicates that although the system does not evolve on the surface \mathcal{Z} where the sagittal and lateral dynamics are decoupled, it stays "close enough" to this surface so as to effectively decouple the dynamics. As a byproduct of this effective decoupling, the φ - $\dot{\varphi}$ dynamics essentially evolve according to (12). This results in a limit cycle in the lateral plane (see Figure 3), i.e., the biped naturally sways from side-to-side. This is especially interesting since this swaying motion was not enforced, but naturally occurred as a result of the functional Routhian reduction procedure.

We conclude by noting that the proposed control method effectively requires the same sagittal actuation as controlled symmetries alone. The lateral actuation is of a similar

magnitude as that in the sagittal plane. Moreover, as the legs are splayed further inwards, the induced sway lessens and the lateral torque decreases. Therefore, our simulation results suggest that a hipped, point-footed bipedal robot can efficiently walk in three dimensions, especially when the legs are appropriately splayed to bring the centers of mass closer to the middle of the robot.

REFERENCES

- [1] A. D. Ames and R. D. Gregg, "Stably extending two-dimensional bipedal walking to three dimensions," in *26th American Control Conference*, New York, NY, 2007.
- [2] A. D. Ames, R. D. Gregg, E. D. B. Wendel, and S. Sastry, "Towards the geometric reduction of controlled three-dimensional robotic bipedal walkers," in *3rd Workshop on Lagrangian and Hamiltonian Methods for Nonlinear Control (LHMNLC'06)*, Nagoya, Japan, 2006.
- [3] A. D. Ames and S. Sastry, "Hybrid Routhian reduction of hybrid Lagrangians and Lagrangian hybrid systems," in *25th American Control Conference*, Minneapolis, MN, 2006.
- [4] S. H. Collins, M. Wisse, and A. Ruina, "A 3-d passive dynamic walking robot with two legs and knees," *International Journal of Robotics Research*, vol. 20, pp. 607–615, 2001.
- [5] A. Goswami, B. Thuilot, and B. Espiau, "Compass-like biped robot part I : Stability and bifurcation of passive gaits," 1996, rapport de recherche de l'INRIA.
- [6] J. Grizzle, G. Abba, and F. Plestan, "Asymptotically stable walking for biped robots: Analysis via systems with impulse effects," *IEEE Transactions on Automatic Control*, vol. 46, no. 1, pp. 51–64, 2001.
- [7] A. D. Kuo, "Stabilization of lateral motion in passive dynamic walking," *International Journal of Robotics Research*, vol. 18, no. 9, pp. 917–930, 1999.
- [8] J. E. Marsden and T. S. Ratiu, *Introduction to Mechanics and Symmetry*, ser. Texts in Applied Mathematics. Springer, 1999, vol. 17.
- [9] T. McGeer, "Passive dynamic walking," *International Journal of Robotics Research*, vol. 9, no. 2, pp. 62–82, 1990.
- [10] B. Morris and J. W. Grizzle, "A restricted Poincaré map for determining exponentially stable periodic orbits in systems with impulse effects: Application to bipedal robots," in *44th IEEE Conference on Decision and Control and European Control Conference*, Seville, Spain, 2005.
- [11] S. Sastry, *Nonlinear Systems: Analysis, Stability and Control*. Springer-Verlag, 1999.
- [12] M. W. Spong and F. Bullo, "Controlled symmetries and passive walking," *IEEE Transactions on Automatic Control*, vol. 50, no. 7, pp. 1025–1031, 2005.

$$\begin{aligned} \frac{d}{dt} \frac{\partial \text{Rem}}{\partial \dot{\theta}_i} &= \ddot{\theta}^T \frac{M_{\varphi,\theta}(\theta)^T M_{\varphi,\theta}(\theta)}{m_{\varphi}(\theta)} e_i + \dot{\theta}^T \frac{\frac{d}{dt}(M_{\varphi,\theta}(\theta))^T M_{\varphi,\theta}(\theta)}{m_{\varphi}(\theta)} e_i + \dot{\theta}^T \frac{M_{\varphi,\theta}(\theta)^T \frac{d}{dt}(M_{\varphi,\theta}(\theta))}{m_{\varphi}(\theta)} e_i - \frac{d}{dt}(m_{\varphi}(\theta)) \dot{\theta}^T \frac{M_{\varphi,\theta}(\theta)^T M_{\varphi,\theta}(\theta)}{m_{\varphi}(\theta)^2} e_i \\ &\quad + \dot{\varphi} M_{\varphi,\theta}(\theta) e_i + \dot{\varphi} \frac{d}{dt}(M_{\varphi,\theta}(\theta)) e_i + \frac{\lambda(\varphi) \frac{d}{dt}(m_{\varphi}(\theta))}{m_{\varphi}(\theta)^2} M_{\varphi,\theta}(\theta) e_i - \frac{\frac{d}{dt}(\lambda(\varphi))}{m_{\varphi}(\theta)} M_{\varphi,\theta}(\theta) e_i - \frac{\lambda(\varphi)}{m_{\varphi}(\theta)} \frac{d}{dt}(M_{\varphi,\theta}(\theta)) e_i \end{aligned} \quad (13)$$

$$\begin{aligned} \frac{\partial \text{Rem}}{\partial \theta_i} &= 2\dot{\theta}^T \frac{\frac{\partial}{\partial \theta_i}(M_{\varphi,\theta}(\theta))^T M_{\varphi,\theta}(\theta)}{2m_{\varphi}(\theta)} \dot{\theta} - \dot{\theta}^T \frac{\frac{\partial}{\partial \theta_i}(m_{\varphi}(\theta)) M_{\varphi,\theta}(\theta)^T M_{\varphi,\theta}(\theta)}{2m_{\varphi}(\theta)^2} \dot{\theta} + \frac{1}{2} \frac{\partial}{\partial \theta_i}(m_{\varphi}(\theta)) \dot{\varphi}^2 + \dot{\varphi} \frac{\partial}{\partial \theta_i}(M_{\varphi,\theta}(\theta)) \dot{\theta} \\ &\quad + \frac{\frac{\partial}{\partial \theta_i}(m_{\varphi}(\theta)) \lambda(\varphi)}{m_{\varphi}(\theta)^2} M_{\varphi,\theta}(\theta) \dot{\theta} - \frac{\lambda(\varphi)}{m_{\varphi}(\theta)} \frac{\partial}{\partial \theta_i}(M_{\varphi,\theta}(\theta)) \dot{\theta} - \frac{1}{2} \frac{\frac{\partial}{\partial \theta_i}(m_{\varphi}(\theta)) \lambda(\varphi)^2}{m_{\varphi}(\theta)^2} \end{aligned} \quad (14)$$

$$\frac{d}{dt} \frac{\partial \text{Rem}}{\partial \dot{\varphi}} = \frac{d}{dt}(M_{\varphi,\theta}(\theta)) \dot{\theta} + M_{\varphi,\theta}(\theta) \ddot{\theta} + m_{\varphi}(\theta) \ddot{\varphi} + \frac{d}{dt}(m_{\varphi}(\theta)) \dot{\varphi} \quad (15)$$

$$\frac{\partial \text{Rem}}{\partial \varphi} = -\frac{\frac{\partial}{\partial \varphi}(\lambda(\varphi))}{m_{\varphi}(\theta)} M_{\varphi,\theta}(\theta) \dot{\theta} + \frac{\lambda(\varphi) \frac{\partial}{\partial \varphi}(\lambda(\varphi))}{m_{\varphi}(\theta)} \quad (16)$$

APPENDIX

In this appendix, we prove Theorem 1. It is, therefore, necessary to investigate the Euler-Lagrange equations of L_λ and how they relate to the Euler-Lagrange equations of L_{fct} .

First note that we can write

$$L_\lambda(\theta, \varphi, \dot{\theta}, \dot{\varphi}) = L_{\text{fct}}(\theta, \dot{\theta}) + \text{Rem}(\theta, \varphi, \dot{\theta}, \dot{\varphi})$$

where

$$\begin{aligned} \text{Rem} &= \frac{1}{2} \dot{\theta}^T \frac{M_{\varphi,\theta}(\theta)^T M_{\varphi,\theta}(\theta)}{m_{\varphi}(\theta)} \dot{\theta} + \frac{1}{2} m_{\varphi}(\theta) \dot{\varphi}^2 \\ &\quad + \dot{\varphi} M_{\varphi,\theta}(\theta) \dot{\theta} - \frac{\lambda(\varphi)}{m_{\varphi}(\theta)} M_{\varphi,\theta}(\theta) \dot{\theta} + \frac{1}{2} \frac{\lambda(\varphi)^2}{m_{\varphi}(\theta)}. \end{aligned}$$

Therefore,

$$\frac{d}{dt} \frac{\partial L_\lambda}{\partial \dot{\theta}_i} - \frac{\partial L_\lambda}{\partial \theta_i} = \frac{d}{dt} \frac{\partial L_{\text{fct}}}{\partial \dot{\theta}_i} - \frac{\partial L_{\text{fct}}}{\partial \theta_i} + \frac{d}{dt} \frac{\partial \text{Rem}}{\partial \dot{\theta}_i} - \frac{\partial \text{Rem}}{\partial \theta_i} \quad (17)$$

$$\frac{d}{dt} \frac{\partial L_\lambda}{\partial \dot{\varphi}} - \frac{\partial L_\lambda}{\partial \varphi} = \frac{d}{dt} \frac{\partial \text{Rem}}{\partial \dot{\varphi}} - \frac{\partial \text{Rem}}{\partial \varphi} \quad (18)$$

where $i = 1, \dots, n = \dim(S)$.

By direct calculation, the various derivatives of Rem are given as in (13), (14), (15) and (16), where in these equations, e_i is the i^{th} standard basis vector for \mathbb{R}^n . The goal is to show that the Euler-Lagrange equations for Rem are satisfied when the functional conserved quantity given in (3) is satisfied.

Note that for $\dot{\varphi}$ satisfying (3), it follows that:

$$\begin{aligned} \ddot{\varphi} &= \frac{\frac{d}{dt}(m_{\varphi}(\theta))}{m_{\varphi}(\theta)^2} M_{\varphi,\theta}(\theta) \dot{\theta} - \frac{\frac{d}{dt}(m_{\varphi}(\theta))}{m_{\varphi}(\theta)^2} \lambda(\varphi) \\ &\quad + \frac{\frac{d}{dt}(\lambda(\varphi))}{m_{\varphi}(\theta)} - \frac{\frac{d}{dt}(M_{\varphi,\theta}(\theta))}{m_{\varphi}(\theta)} \dot{\theta} - \frac{M_{\varphi,\theta}(\theta)}{m_{\varphi}(\theta)} \ddot{\theta}. \end{aligned} \quad (19)$$

Moreover, substituting (3) and (19) into (13), it is easy to verify that:

$$\left. \frac{d}{dt} \frac{\partial \text{Rem}}{\partial \dot{\theta}_i} \right|_{J(\theta, \varphi, \dot{\theta}, \dot{\varphi}) = \lambda(\varphi)} = 0,$$

and substituting (3) into (14) yields:

$$\left. \frac{\partial \text{Rem}}{\partial \theta_i} \right|_{J(\theta, \varphi, \dot{\theta}, \dot{\varphi}) = \lambda(\varphi)} = 0.$$

Therefore,

$$\left[\frac{d}{dt} \frac{\partial \text{Rem}}{\partial \dot{\theta}_i} - \frac{\partial \text{Rem}}{\partial \theta_i} \right] \Big|_{J(\theta, \varphi, \dot{\theta}, \dot{\varphi}) = \lambda(\varphi)} = 0, \quad (20)$$

for $i = 1, \dots, n$.

Now, we clearly have that

$$\frac{d}{dt}(\lambda(\varphi)) = \frac{\partial}{\partial \varphi}(\lambda(\varphi)) \dot{\varphi} = \frac{\partial \text{Rem}}{\partial \varphi} \quad (21)$$

for $\dot{\varphi}$ satisfying (3). Therefore, substituting (3), (19) and (21) into (15) and (16), it is easy to verify that:

$$\left[\frac{d}{dt} \frac{\partial \text{Rem}}{\partial \dot{\varphi}} - \frac{\partial \text{Rem}}{\partial \varphi} \right] \Big|_{J(\theta, \varphi, \dot{\theta}, \dot{\varphi}) = \lambda(\varphi)} = 0. \quad (22)$$

We now have the framework in which to prove Theorem 1.

Proof: [of Theorem 1] (\Rightarrow) Let $(\theta(t), \varphi(t), \dot{\theta}(t), \dot{\varphi}(t))$ be a flow of the vector field f_{L_λ} on $[t_0, t_F]$ with $\dot{\varphi}(t_0)$ satisfying (4) and let $(\bar{\theta}(t), \bar{\theta}(t))$ be a flow of the vector field $f_{L_{\text{fct}}}$ on $[t_0, t_F]$ with $\bar{\theta}(t_0) = \theta(t_0)$ and $\bar{\theta}(t_0) = \dot{\theta}(t_0)$. In addition, let $\bar{\varphi}(t)$ be a curve satisfying

$$\begin{aligned} \bar{\varphi}(t_0) &= \varphi(t_0), \\ \dot{\bar{\varphi}}(t) &= \frac{1}{m_{\varphi}(\bar{\theta}(t))} (\lambda(\bar{\varphi}(t)) - M_{\varphi,\theta}(\bar{\theta}(t)) \dot{\bar{\theta}}(t)). \end{aligned}$$

By (17), (18), (20) and (22), it follows that the curve $(\bar{\theta}(t), \bar{\varphi}(t), \dot{\bar{\theta}}(t), \dot{\bar{\varphi}}(t))$ satisfies the Euler-Lagrange equations for L_λ , and is thus a flow of the vector field f_{L_λ} on $[t_0, t_F]$. By the uniqueness of solutions to f_{L_λ} , it follows that

$$(\theta(t), \varphi(t), \dot{\theta}(t), \dot{\varphi}(t)) = (\bar{\theta}(t), \bar{\varphi}(t), \dot{\bar{\theta}}(t), \dot{\bar{\varphi}}(t))$$

since these curves have the same initial condition. Therefore, $(\theta(t), \dot{\theta}(t))$ is a flow of the vector field $f_{L_{\text{fct}}}$ on $[t_0, t_F]$ and $\dot{\varphi}(t)$ satisfies (5).

(\Leftarrow) Let $(\theta(t), \dot{\theta}(t))$ be a flow of the vector field $f_{L_{\text{fct}}}$ on $[t_0, t_F]$ and $(\varphi(t), \dot{\varphi}(t))$ a pair satisfying (5). Therefore, by (17), (18), (20) and (22), it follows that the Euler-Lagrange equations for L_λ are satisfied since the curve $(\theta(t), \dot{\theta}(t))$ satisfies the Euler-Lagrange equations for L_{fct} by definition. Therefore, $(\theta(t), \varphi(t), \dot{\theta}(t), \dot{\varphi}(t))$ is a solution to f_{L_λ} on $[t_0, t_F]$ satisfying (4). \blacksquare